A DFT study of structural and thermal properties of 2D layers (Short Title: Two-Dimensional Materials)

Abdul Majid[1,*], Hajra Kanwal[1], Salah Ud-Din Khan[2], Ashfaq Ahmad[3]

[1]Department of Physics, University of Gujrat, Gujrat 50700, Pakistan
[2]Sustainable Energy Technologies (SET) Center, College of Engineering, King Saud University, PO-Box 800, Riyadh, 11421, Saudi Arabia
[3]Department of Chemistry, College of Science, King Saud University Riyadh, P.O.Box 2455, Riyadh-11451, Kingdom of Saudi Arabia

*Correspondence: Abdulmajid40@yahoo.com Telephone: +923328009610

Abstract

Two-dimensional (2D) materials are known to owe exceptional properties which are prerequisites for the future applications. Despite significant efforts and unprecedented achievements to realize resourceful beyond-graphene 2D materials, the comprehensive knowledge on such materials is lacking due to which several device grade applications are still in pipeline. This work was carried out with motivation to investigate the thermal stability of contemporary 2D mono-layered materials including graphene, borophene, aluminene, germanene, BN, SiC and MoS_2 using Molecular Dynamics simulations. The thermal broadening, bond breakage and bond formation for the slabs are analyzed on the basis of radial distribution function (RDF). It is found that several materials out of the list are capable to withstand high temperatures depicting the essential thermal stability. The values of thermal stability of the materials were compared by plotting the temperature and energy curves whereas phase transition temperature and heat capacity of the slabs were found by taking germanene as benchmark. The phase transition temperatures are found as 4510 K, 2273 K, 933 K, 1670 K, 3246 K, 4050 K, and 1460 K for graphene, borophene, aluminene, germanene, BN, SiC and MoS_2 respectively.

Keywords: ReaxFF, Molecular Dynamics, RDF, phase-transition

1. Introduction

Two-Dimensional (2D) materials are atomically thick sheets in the form of elemental layers or hetero-layers assembled via Van der Waals interactions. These materials are in limelight due to their exceptional electronic, mechanical, transport and surface properties which are not available in their bulk counterparts. The research and industrial activities related to 2D-materials have drawn the increasing attention after successful invention of graphene-monolayer owing to the mentioned potentials for future applications (Ma, N., Reis, M.S., 2017), (Balendhran, Walia, Nili, Sriram, & Bhaskaran, 2015). The restricted capability of

graphene on account of its zero-band gap has initially put exploration of graphene-like materials on the track. The synthesis of beyond-graphene (Balandin et al., 2008) 2D materials including group IV-IV as SiC (Pan et al., 2011), Silicene (Vogt et al., 2012) and Germanene (Dávila, Xian, Cahangirov, Rubio, & Le Lay, 2014)), group III-V (J. Wang, Ma, Liang, & Sun), Aluminene, black-phosphorene (Liu et al., 2014) and TM-DCs (2h-MoS_2) in recent past has triggered a lot of related research throughout the globe.

There is great quest of 2D semiconducting materials having in-plane strong covalent bonds that can resist against the temperature variations and strong mechanical deformations. Besides this, there is great demand of such plane materials that could exhibit graphene-like-flatness due to the observed out-of-plane buckling in majority of the explored structures (Chen et al., 2013). The 2D graphite was first studied way back when Wallace worked using 'tight binding' method to study the electronic band structure (Wallace, 1947) while graphene was successfully synthesized in 2004 (Chen et al., 2013), (Hill, Geim, Novoselov, Schedin, & Blake, 2006) and got overwhelming attention in 2D materials due to its extensive applications (Geim & Novoselov, 2010), (Neto, Guinea, Peres, Novoselov, & Geim, 2009)**.** These materials with hexagonal honeycomb lattice have been found suitable for applications in opto-electronics and spintronics due to their apposite band structure (Kroto, 1990)**,** (Blake et al., 2007). In recent past, silicene (Davydov, 2010) and germanene (Dávila et al., 2014) earned extensive research interest. The lattice constant of germanene for hexagonal crystal lattice is 4.03Å (Lebegue & Eriksson, 2009) which is higher than that of graphene (2.46Å) on the account of differences in ionic radii. The molecular dynamics investigation of germanene suggests that it is very stable structure (Giang, Tran, & Van Hoang, 2019). Further, unlike graphene, the germanene has exhibited spin-orbit coupling and quantum hall effect. Borophene is another 2D-material which was predicted first time in 2012, (Zhang, Yang, Gao, & Yakobson, 2015) and later successfully synthesized (Feng et al., 2016).

The investigation of mechanical, electronic and optical properties of 2D materials have been routinely studied using first principles strategies (Lherbier, Botello-Méndez, & Charlier, 2016). Borophene comprises planar as well as striped buckled structure among which trigonal planar structure with vacancies on hexagonal sites is more stable (X. Yang, Ding, & Ni, 2008). The neoteric discovery of borophene has provoked the community to explore similar materials including aluminene (Kamal, Chakrabarti, & Ezawa, 2015). The buckled structure of aluminene has been found stable and exhibited metallic behavior as per reported first principles calculations (Junhui Yuan, Yu, Xue, & Miao, 2017). In addition to borophene and aluminene the quest for further 2D materials have resulted into discovery of materials of group-V which have been found suitable for applications as in solar cells (Huang et al., 2018), gas-sensors**,** field-effect transistors (Kou, Frauenheim, & Chen, 2014) and as anode in

lithium-ion batteries (Li, Yang, Zhang, & Zhang, 2015). Similarly, the elemental 2D-materials and heterostructures from group IV-IV (SiC), group III-V(2h-BN) and TMDCs have been predicted and successfully synthesized. 2D SiC is a promising material due to its mechanical and thermal stability as well as chemical-inertness. The bonds in SiC layer are of sp^2 hybrid character rather than sp^3 hybridization and its structure can be viewed as silicene or graphene with the additional Si or C atoms (Şahin et al., 2009). The graphene-like flat structure of 2D SiC offers a band gap of 2.25 eV and is known to be thermally or mechanically strong material.

The monolayer of hexagonal-BN exhibits the same lattice as that of graphene but with a small lattice-mismatch of about 1.7% (J. Wang, Ma, & Sun, 2017)**.** Boron and nitrogen make ionic-bonds rather than covalent-bonds between carbon atoms as in graphene (Golberg et al., 2010). 2D-BN is an insulator exhibiting wide band gap and illustrates tremendous thermal and mechanical stability as per molecular dynamics. Owing to the properties, it shown functionality in nano and micro devices (Hernandez, Goze, Bernier, & Rubio, 1998), (Zhi, Bando, Tang, Kuwahara, & Golberg, 2009)**.** Similarly single-layer 2H-phase of MoS_2 with direct band gap has recently been discovered with the remarkable applications in opto-electronic devices (Q. Wang, Kalantar-Zadeh, & Kis, 2012). 2D-sheet of MoS_2 comprises of triple planes in which a layer of Mo atoms is sandwiched between two layers of S atoms as S_{top}-Mo-S_{bottom}. MoS_2 is found interesting due to its polymorphism as it exhibits 2H (semi-conducting) and 1T (metallic) phase owing to the arrangement of S-atoms (Wypych & Schöllhorn, 1992). 2H-phase of MoS_2 is found very stable at high temperatures while employing molecular dynamics analysis.

The majority of studies on the mentioned 2D materials are related to their applications at ambient conditions. However, less is known on functionality of these materials under extreme conditions of temperature, pressure and radiations. The current study was aimed at investigation of structural properties and temperature dependent phase stability of present-day 2D materials using molecular dynamics (Aktulga, Pandit, van Duin, & Grama, 2012).

2. Computational details

MD simulation has been commonly employed to model the physical conditions of materials on the basis of ab-initio methods. The simulation helps determining the kinetic and thermo-dynamic properties of system by using equations of motion. The MD operates using Newton's equations of motion to calculate the interatomic forces and time evolution of geometries. The deviation from the original trajectory may be based on approximations and give rise to numerical errors (Frenkel & Smit, 2002). The ensembles for physical configurations to study the time averages such as temperature, density and free energies are

usually carried out (Patti, 2010). Temperature dependent MD is very useful to understand the conditions for break-down of crystallinity in the materials. This study involves comprehensive investigation of the structural properties of 2D-materials based on the radial distribution function calculated through MD.

In this work, ReaxAms (reactive Amsterdam Modeling Suite) was used to perform the MD simulations at different temperature ranges varied from material to material. To study the structural stability of 2D-materials the simulations were carried out using 6x6 supercell starting from optimized unit cells of the structures. The initial geometry was relaxed by using conjugate-gradient method and energy is minimized to its local-minimum value with Nose-hoover chains having length of about 10. The Brendsen thermostats and barostats to control the temperature and pressure with the time steps of ΔT=0.1 fs was employed. The number of steps/iterations as 150000 were found large enough such that the simulation can get enough time to equilibrate properly. The sample frequency was set to 45 Hz and velocities were initialized randomly. The Newton's equations of motion were integrated by using standard method of velocity-verlet algorithm. The time step for all the simulation was set to be 0.25 fs.

Radial-distribution function (RDF) is a resourceful tool to examine the structural information of materials which can be calculated by estimating the distance amongst all pairs of atoms. Fourier transform of radial distribution curve is used for the static factor attained through x-ray crystallography. The probability of finding an atom is determined using (2),

$$¿ n_{\alpha,\beta}(r.r+\Delta r) \geq \rho_\beta 4\pi^2 g_{\alpha,\beta}(r)\Delta r \ldots\ldots\ldots (2)$$

Where $\rho_\beta = N_\beta$/V and $g_{\alpha,\beta}(r)\Delta r$ is RDF which is proportional to the probability of finding an atom between distance r and $r+\Delta r$. RDF for 2D-materials is given as

$$g_{AB}(r) = \frac{\Delta n_{AB}}{2\pi r \Delta r \rho_B} \ldots\ldots\ldots (3)$$

Where ρ_B is the average-density of B atoms and Δn_{AB} is average-number of particles of B atoms present in the region between r and $r+\Delta r$. The RDF ought to be delta-function at T=0K whose integral over the real-line is one but as temperature rises the delta function transformed into smooth-Gaussian-peaks. The structural properties were studied using radial distribution function RDF at every temperature.

The reactive force field potential contains three types of interactions (coulomb, van der Waals and electrostatic repulsion energies) so total energy can be calculated as change in the energy in collection of atoms when they are bonded. In this work, we used the ReaxFF (Ostadhossein et al., 2017) bond order potential to represent the interactions between atoms of all mono-

layered materials. ReaxFF is a versatile tool to study the atomic interactions (Yoon, Ostadhossein, & Van Duin, 2016). The energy of system is calculated in ReaxFF as

$$E_{system} = E_{bond} + E_{val} + E_{tor} + E_{¿} + E_{under} + E_{lp} + E_{vdw} + E_{coloumbic} \ldots\ldots\ldots (1)$$

The sum of valence-angle, torsion-angle, lone-pair energy, bond energy, columbic energy, over-coordinate, under-coordinate and distance dependent van-der-Waals energy.

3. Results and discussion

The accuracy of structural parameters of the studied materials were ensured by matching the calculated values of lattice-constant, bond-length and dihedral angles with reported values. Further, the analysis of temperature-energy variations, the thermal broadening is also carried out and discussed to examine the thermal-stability for usage of the materials in high temperature applications. The calculated results exhibiting structural and thermal stability of the materials at wide range of temperatures are described in the following sections.

3.1. Structural properties

The MD properties of 2D-monolayered studied via ReaxAMS to shed light on temperature dependent behavior, structure and thermal stability are described herein. As the temperature is increased the structures become rippled which produced out-of-plane fluctuations owing to motion of atoms in the structure. The crystalline structure of sheet is maintained at room temperature but the structures become rippled with increase in temperature depending on phase transition. If the structure resists against high temperature to have high melting-temperature, it can exhibit long-range crystallinity. Graphene is thermally most stable material as its hexagonal structure endures at temperature up-to 3000-4000 K beyond which the bonds start to break and structure disrupts at 6000 K. Similarly, the other mentioned materials start facing the ripples in their structure at a specific temperature.

Germanene is found in honeycomb pattern with low-buckling instead of planar structure. which is one of its stable geometry. The germanene has largest ionic-radius among its group members and adopts mixed sp^3- and sp^2-hybridization (Giang et al., 2019). The computed value of lattice constant a is 3.97 Å and can be varied from 3.97-4.01 as shown in the table 1. The average value of bond-length between Ge-Ge atoms in the honeycomb lattice is calculated as 2.51 Å which is closely related to literature (Cahangirov, Topsakal, Aktürk, Şahin, & Ciraci, 2009) value. The buckling-amplitude for free-standing germanene is determined whose value is 0.7 Å as shown in the figure 1. The majority of 2D materials are buckled, the optimized structure of germanene given in figure 1 is shown here as a representative structure.

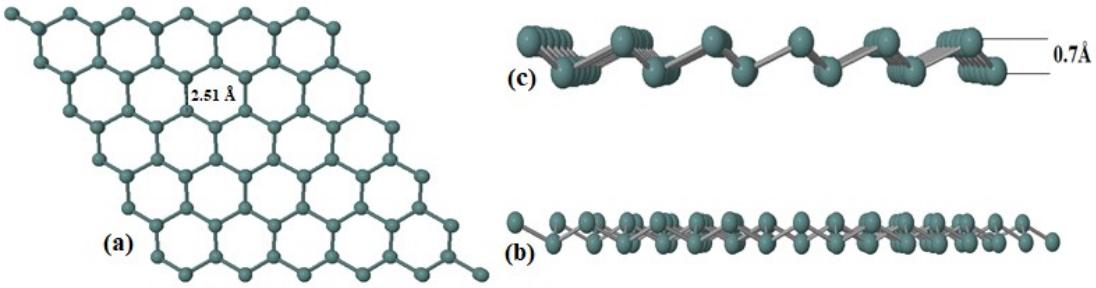

Figure 1: The optimized structure of buckled germanene viewed along (a) z-axis, (b) y-axis and (c) x-axis. The calculated values of bond length and buckling width are shown.

Graphene, aluminene, h-BN and SiC monolayers adopt sp^2-hybridization. In case of graphene the carbon atoms are packed in planar-honeycomb pattern with electronic-resonance and delocalization as responsible for its stable structure. The out-of-plane $2p_z$ orbitals of C atoms overlap with each other to develop π-bonding in order to facilitate delocalization of electrons. In contrast the in-plane 2s orbitals form strong covalent σ-bonding with $2p_x$ and $2p_y$ orbitals of C atoms (G. Yang, Li, Lee, & Ng, 2018). The computed results reveal that the bond length between C-C atoms is 1.42Å and lattice constant for the graphene is 2.46 Å which agrees well with reported value (Mukhopadhyay & Behera, 2013) as shown in table 1. Aluminene is geometrically stable in buckled structure in which s, p_x and p_y orbitals overlap to produce strong sp^2-hybridization (Junhui Yuan et al., 2017). The calculated lattice constant is 2.74 Å, and bond-length of Al-Al atoms is seen to be 2.76 which is close to DFT value 2.92 Å (Kamal et al., 2015) shown in table 1. The single-layered h-BN is packed with boron ($2s^22p^1$) and nitrogen atoms ($2s^22p^3$) in sp^2-hybridization with strong in-plane σ-bonds and weak out-of-plane π-bonds (Thomas, Ajith, Chandra, & Valsakumar, 2015). The bond length between B-B, B-N and N-N in optimized structure is 2.511 Å, 1.45 Å, 2.52 Å respectively. The lattice constant a is found to be 0.25 Å as in previously reported literature (J. Wang, Ma, & Sun, 2017).

The SiC monolayer is flat structured which usually makes sp^2-hybridization but preference of Si to adopt sp^3-hybridization opens door to several morphologies with low-buckling (Shi, Zhang, Kutana, & Yakobson, 2015). The bond length calculated between Si-C, C-C and Si-Si atom is 1.78Å, 3.15 Å and 3.5 Å respectively and the lattice-constant of optimized structure is 3.10 Å as studied by Lin (Lin et al., 2013). The structure of alpha boron is triangular planer with hexagonal vacancies in the lattice and bonding is either two-center bonding or three-center bonding depending on the number of electrons in outer-most shell. The single-layered structure of 2h-MoS_2 has triangular-buckled structure in which Mo atoms are sandwiched between two layers of S atoms such as S-Mo-S alternatively. The calculated bond length between Mo-Mo, Mo-S and S-S atoms is 3.2 Å, 2.415 Å and 3.1 Å respectively and the

lattice constant of 2h-MoS2 is found to be 3.15 Å shown in the table 1 which agrees with the DFT results (Sun et al., 2014). The 2h-phase is more stable in which Mo-atoms occupied the triangular-prism lattice between the hexagonal-layers of closely-packed S-atoms. These layers of S and Mo atoms are interconnected through weak van-der-Waals forces (Ostadhossein et al., 2017).The optimized structures of the mentioned 2D-materials are shown in figure 2 whereas the calculated structural parameters including bond length, lattice constant, crystal structure, band gap and electronic properties are given in table 1.

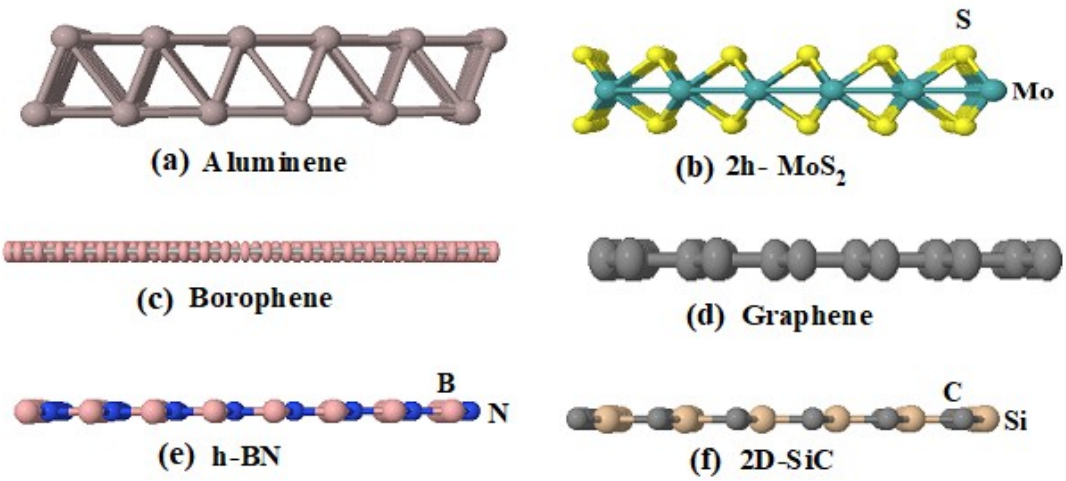

Figure 2: The optimized structures of Aluminene, 2h-MoS2, Borophene, Graphene, h-BN, and 2D-SiC viewed along x-axis

Table 1: Structural properties of 2D materials depicting the crystal structure, band gap, bond-length, lattice-parameters and symmetry

Materials	Crystal structure	Lattice constant (a) in Å	Bond length (Å)		Band gap (eV)	Conductivity
2D-SiC	Hexagonal-planar	3.10	C-C C-Si Si-Si	3.15 1.78 3.5	2.52	Semi-conductor
Graphene	Hexagonal-planar	2.46	1.42		0	Semi-metal
Borophene	Triangular with periodic h-vacancies (α_5)	4.37	1.8		2	Semi-metal
			Mo-Mo	3.2		

2h-MoS_2	Triangular-buckled	3.15	Mo-S S-S	2.145 3.1	1.6	Semi-conductor
h-BN	Hexagonal-planar	0.25	B-B B-N N-N	2.511 1.45 2.65	5.9	Insulator/ semi-conductor
Aluminene	Buckled	4.486	2.59		1.618	Semi-metal
Germanene	Triangular-buckled	3.97	2.45		0.26	Semi-metal

3.2. Thermal properties

3.2.1. Radial-Distribution Function

The RDF calculated for the mentioned 2D materials in order to shed light on structural modifications at different temperatures are described below.

(i) 2D-SiC

RDF calculated for 2D-SiC monolayer in temperature ranges from 100-4500 K is shown in figure 3. The peaks of C-C bonds at low temperature (100-800 K) are sharp and intensified, characterize the crystalline structure but as the temperature rises the peaks turn out to be wide and dumpy by slightly changed position of peaks depicts the high stability of SiC. At high temperature (>800 K) the peaks grow broader due to rapid vibrations of atoms in equilibrium, the structure drops its crystallinity and becomes amorphous owing to decline in short-range order (SRO). The bond length of first peak is about 3.1Å amongst C-C atoms which is nearly equal to the peak position in diamond (2.55Å). The existence of weak bonding in buckled structures increased the intensity of the peaks.

The C-Si peaks stay persistent throughout the entire simulation with fixed central position (1.789 Å) and slight thermal expansion. Accompanied by temperature changes the peaks get their shapes accordingly. Similar to C-C peaks these as well get broader and smaller in height, lose their ordered structure as temperature rises and vice versa. There is oscillating RDF for 2D-materials even at large separations but it decays after one or two shells in amorphous materials. The 2D-SiC contains homo-nuclear as well as hetero-nuclear bonds (C-Si) epitomize no segregation of silicon and carbon atoms during the simulation.

The RDF peak of Si-Si bond is found at 3.5Å but as the temperature increases, bond length increases slightly which shows the rapid movement of atoms attribute to higher kinetic energy at equilibrium position and thermal broadening. At temperature ≤1500 two distinctive peaks exist in the structure but if temperature rises from 1500 K, first peak shifts apart and slightly

widen while second peak diminishes. The probability G(r) between two peaks is non-zero and remains constant beyond 8 Å depicts the slight change in radial distribution function at higher temperature ≥1500 K. The sheet of SiC remains stable at 2000 K and maintain its hexagonal structure although there are some ripples and out of plane fluctuations when viewed from the side while heating from 100 K to 4500 K. If temperature is medium-low the probability G(r) is zero between the first and second nearest neighbor peak in all bonds of SiC illustrates the specific geometry of structure.

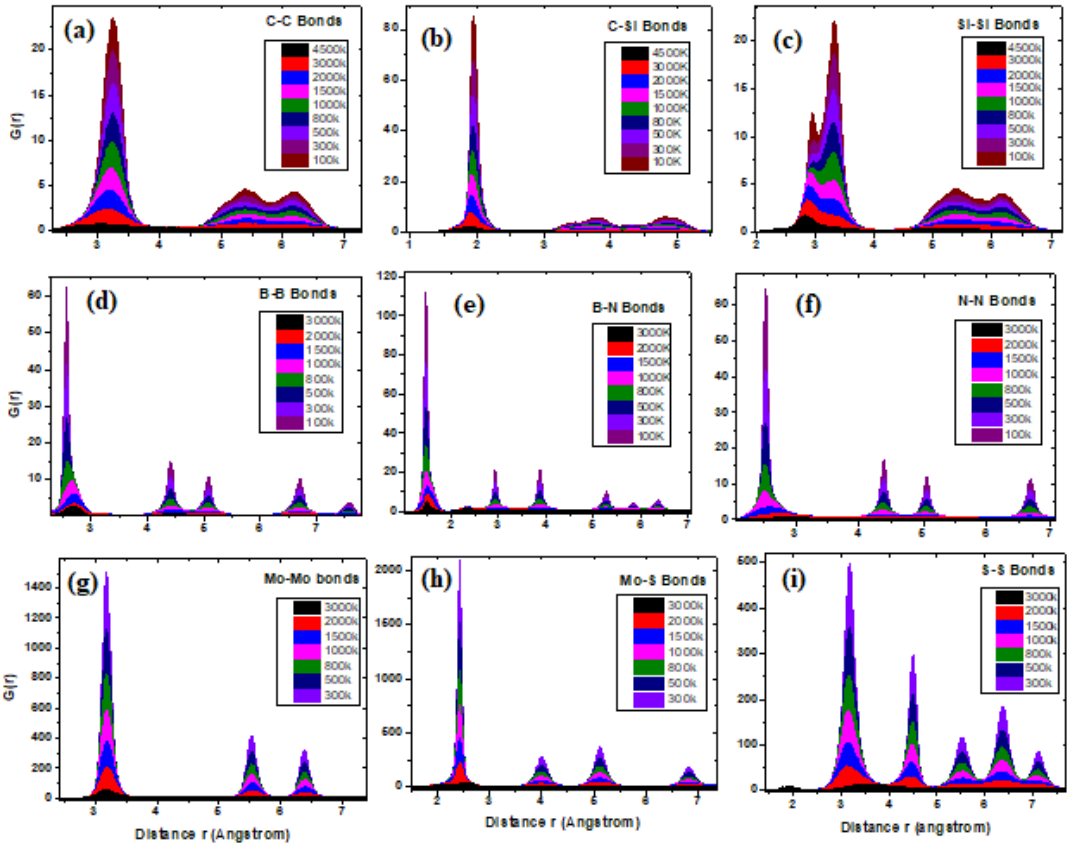

Figure 3: RDF-peaks of mono-layered compound materials as a function of interatomic distance between atoms of (a,b,c) 2D-SiC at temperature ranges from 100 to 4500 K (d,e,f) h-BN at temperature ranges from 100 to 3000 K (g,h,i) 2h-MoS_2 at temperature ranges from 300 to 3000 K

(ii) h-BN

The RDF-peaks calculated for h-BN sheet are displayed in figure 3 which shows peak positions of B-B, B-N and N-N are 2.511Å, 1.45 Å and 2.65 Å. The distance of peaks increases nearly from 2.511 to 2.53 but for the B-N and N-N bonds the distance decreases slightly from 1.45 Å to 1.4 Å and 2.65 Å to 2.5 Å respectively as in the increase of temperature. The greater or smaller distances represent the thermal broadening of peaks which depend on the motion of atoms. The RDF-peaks depict the distance between atoms which can also be calculated by using other techniques as geometry-analysis (Jianhui Yuan & Liew, 2014),

(Thomas et al., 2015) With the increase in temperature the atoms move from their equilibrium-position as a result which the probability of finding particles in distance r decreases. There exists a coupling in the h-BN and SiC mono-layered sheets which corresponds to temperature-independent coupling distance in B-N and 2D-SiC. Moreover, in h-BN the position of first radial-distribution peak of B-B, B-N, and N-N is nearly double that of Si-Si, Si-C, and C-C in mono-layered sheet of SiC respectively.

(iii) 2h-MoS_2

The RDF-peaks calculated for 2h-MoS_2 at temperature ranges from 300-3000 K are shown in figure 3. The peaks of Mo-Mo, Mo-S, and S-S are found at the distance of 3.2 Å, 2.415 Å, and 3.1 Å respectively. The peaks positions shift as temperature increases further, wherein the Mo-Mo, S-S and Mo-S peaks shift towards left (decreasing distance) slightly. At temperature between 2000 and 3000 K the most of the bonds in the structure break down which represent the liquid state of structure (Ahadi, Shadman Lakmehsari, Kumar Singh, & Davoodi, 2017). It is shown from the results SiC is most stable against temperature variations because it resists the temperature even at 4500k as its melting point is about 4050k after which RDF peaks diminish due to thermal broadening and bond breakage and structure is converted to liquid state. The melting point of h-BN is 3246 K makes it second most stable and 2h-MoS_2 corresponds to least stable among compounds. It is predicted below from the most to least stable depending upon their melting point and structural configuration: 2D-SiC (4050K)>h-BN (3246K)>2h-MoS_2 (1460K). Thermal stability can be compared by calculating full-width half maxima (FWHM) at a specific temperature.

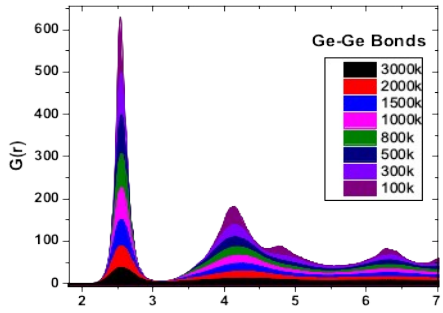

Figure 4: RDF- peaks of Germanene as a function of inter-atomic distance (r) at x-axis and probability G(r) at y-axis

Figure 4 depicts the RDF of germanene at certain temperatures from 100-3000 K and this is considered as reference for other materials as its RDF-peaks has accurately reported in recent past (Giang et al., 2019). The temperature above 1000 K structure is relatively smooth with low-broadened and reduced peaks predicts that germanene structure have lost its long-range

crystallinity and well-atomic arrangement. It divulges at higher temperature above 1000 K the germanene unveils the liquid-state. Then phase-transition occurs between temperatures 1000-1500 K where the RDF peaks become smooth so the crystallization-temperature of germanene is 1340 K as reported earlier (Giang et al., 2019). At low temperature, the germanene shows its crystalline structure with sharp RDF-peaks. The RDF-peaks are found at the distance of 2.45 Å which is the average bonding distance between Ge-Ge bonds in its crystalline structure. The melting or phase-transition temperature of germanene is 1670 K (Giang, Van Hoang, & Hanh, 2020) which shows the thermal stability of germanene at much higher temperatures of about 1500-2000 K and above to some extent.

The RDF-peaks of some other elemental mono-layered materials are shown in figure 5. To check the long-range crystallinity in graphene RDF-peaks of graphene are also shown in figure 5. The RDF of graphene is oscillatory even after at high temperatures while the oscillations vanish after one or two shells. The structure stability is defined through reduction in the height of RDF-peaks at higher temperatures. For the perfect liquid state of material, the crystal loses its long-range order due to thermal broadening and peaks-height is abridged to zero. The nearest (first)-neighbor inter-atomic distance in C-C atoms is 1.42 Å which is closely equal to bond-length between C-C atoms in graphite (1.46 Å) at lower temperature, but peaks get broader and declined at C-C distance of approximately 1.3 Å. The melting temperature of graphene ranges from 4000-6000 K but the theoretically reported melting temperature of graphene is 4510 K (Ganz, Ganz, Yang, & Dornfeld, 2017) showing that after this temperature the bonds between C-C atoms start decaying and thermal broadening occurs. But at 6000k the atoms completely break their bonds, peaks height approaches to zero and they move farther apart from each other left the structure disrupted. So graphene is thermally stable at temperature up-to 5000 K.

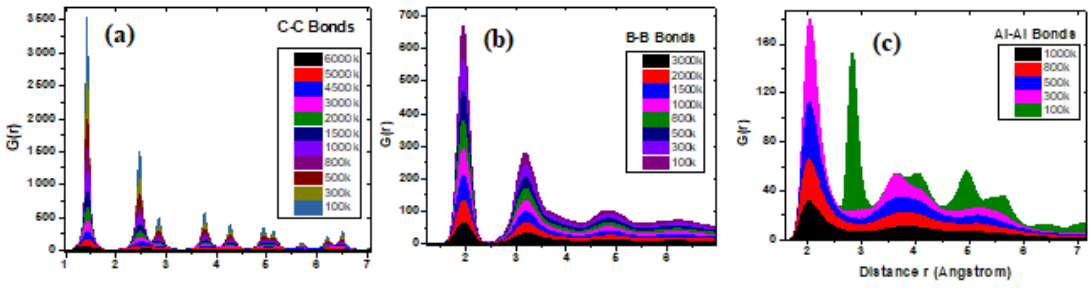

Figure 5: RDF-peaks of mono-layered elemental materials as a function of interatomic-distance of (a) Graphene at temperature ranges from 100 to 6000 K (b) Borophene at temperature ranges from 100 to 3000 K and (c) Aluminene at temperature ranges from 100 to 1000 K

The RDF-peaks of alpha borophene are shown in figure 5 which is thermally very stable as compared to its other crystal structures (striped borophene). Although no such thermal stability through molecular dynamics on borophene is reported yet but borophene is proved to

be thermally very stable through first-principle calculations (Peng et al., 2017). The peak of B-B atom is located at distance of nearly 1.8 Å at lower temperatures which is the average-distance between boron atoms in borophene-sheets. Borophene withstands a high temperature range which shows its stability. As the melting temperature of borophene is 2273 K (Ranjan et al., 2019) which shows that borophene shows very stable structure even temperature up-to 2000 K.

The RDF-peaks of buckled aluminene are shown in the figure 5. The buckled structure of aluminene is reported thermally very stable through first-principle study (Junhui Yuan et al., 2017). At 100 K the RDF-peak for aluminene is located at the distance of 2.59 Å which is the average distance between Al-Al atoms in its crystalline form (Kamal et al., 2015). Aluminene is thermally less stable than its other group members as the phase-transition temperature in aluminene is 933 K and it resists the temperature variations about 1000 K after which the structure no-longer remains well-ordered, loses its crystallinity and changes its state from solid to liquid.

Table 2 Stability trend of elemental materials by calculating full-width half-maximum and phase-transition temperatures

Materials	Phase-transition temperature (K)	FWHM (at 3000k)			
		Bonds	First peak	Second peak	Third peak
Graphene	4510	C-C	0.55	1.3	3.48
Borophene	2273	B-B	1.17	2.42	7.30
Germanene	1670	Ge-Ge	1.31	4.87	9.19
Aluminene	933	Al-Al	1.76	5.05	9.32

The stability of different materials is compared by their phase-transition temperature and full-width at half-maximum (FWHM). In the above table from most to least stable elemental materials are given but the compound materials such as 2D-SiC, h-BN, and 2h-MoS_2 do not follow one of above rule of FWHM due to presence of homo-nuclear and hetero-nuclear bonds. The full-width half-maximum of RDF-peaks shows the reliability of any crystal-structure. The more thermally stable the material is, the peaks of RDF are sharper and heightened corresponds to smaller value of FWHM and vice-versa. Table 2 shows the positions of three main peaks of diverse materials which are located at 0.55, 1.3, and 3.48 nm in graphene. Compared these values of FWHM with other materials which are less stable than, so these values faintly narrow-down according to their stability sequence. FWHM value indicate the integrity of crystals as Graphene > borophene > Germanene > Aluminene.

3.2.2. Phase-transition temperature

The temperature dependent total energy (eV/at) values of different 2D-materials up-to certain temperature ranges are shown in figure 6. The energy values point towards a complete behavior of phase-transition in these materials at a specific temperature similar to previously reported results.

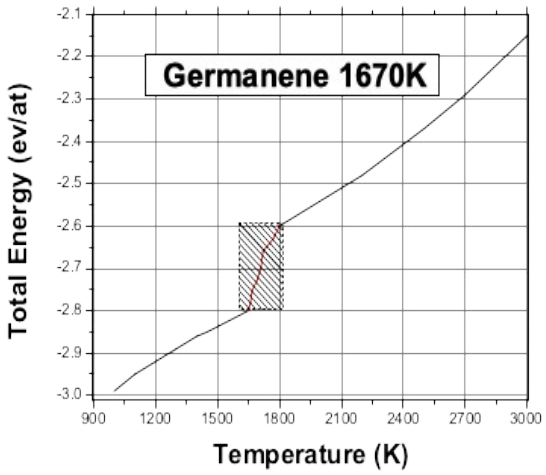

Figure 6: Temperature dependent energy values and their corresponding graph for Germanene.

Initially the values of energy increase linearly as temperature increases i.e. at 1000 K, -2.99 at 1100 K, -2.95 and so on till temperature 1000-1660 K but there is shown a sharp increase in energy-value at about 1670 K where its value is -15.09 but as temperature reaches to 1690 K the value of increases to -14.98 and this trend is followed up-to temperature 1670-1720 K, then it again start to increase linearly but with higher energy values from 1720 to 3000 K or even more than this temperature. Then energy values at temperatures 2200, 2500, 2700 and 3000 K are -2.53, -2.37, -2.19 and -2.15 eV/at respectively.

The curve of this T-E graph is linear at starting temperature representing the solid state of structure but it suddenly changes its behavior at about 1670k which is the phase transition temperature for Germanene, at this temperature the structure starts converting from solid state to liquid state and its energy becomes greater as at high temperatures the atoms collide with each other more vibrantly at their equilibrium position cause the bond-breakage. At temperature 1720K the energy values again start to increase linearly, because of this behavior of energy can be clearly stated that the structure has converted to completely-molten state, containing high amount of energy. The phase-transition curve for germanene closely matches

to literature value so it is considered as a reference material to represent the phase-transition curve for other 2D-materials as well (Giang et al., 2020) .

Table 3: Temperature dependent total energy values (eV/at) of different 2D-materials

Graphene		h-BN		2D-SiC		Borophene		Aluminene		2h-MoS2	
T(K)	E(eV /at)	T(K)	E(eV/ at)	T(K)	E(eV /at)	T(K)	E(eV /at)	T(K)	E(eV /at)	T(K)	E(eV /at)
3000	-6.6	1000	-6.93	1500	-5.87	500	-5.45	200	-3.09	100	-4.98
3500	-6.52	1500	-6.79	2000	-5.69	800	-5.42	300	-3.06	300	-4.92
4500	-6.23	2000	-6.68	2500	-5.52	1000	-5.39	400	-3.02	500	-4.87
5000	-6.07	2500	-6.56	3000	-5.36	1600	-5.34	500	-2.98	800	-4.78
5300	-5.9	3000	-6.43	3500	-5.17	2050	-5.3	650	-2.92	1100	-4.69
5350	-5.5	3100	-6.38	3900	-5.05	2100	-5.29	800	-2.88	1150	-4.62
5400	-5.2	3150	-6.3	4000	-5	2195	-5.26	820	-2.87	1200	-4.59
5550	-4.85	3200	-6.25	4050	-4.9	2200	-5.23	850	-2.84	1300	-4.5
5650	-4.55	3250	-6.21	4100	-4.83	2300	-5.19	870	-2.81	1400	-4.4
6500	-3.81	3300	-6.18	5000	-4.59	2800	-5.12	1200	-2.74	2000	-4.25
7000	-3.6	3500	-6.11	5500	-4.41	3000	-5.08	1500	-2.69	2500	-4
7500	-3.34	3800	-6	6000	-4.27	3200	-5.04	1800	-2.63	3000	-3.76
8000	-3	4200	-5.87	6500	-4.08	3500	-4.97	2000	-2.58	3100	-3.75

T-E graphs extracted for the mentioned 2D-materials are given in figure 7. A linear trend is observed in the start indicating solid-phase but with further increase in temperature an abrupt increase in E is observed at a specific temperature depicting the phase-transition. The energy increases abruptly during transition due to rapid collisions of atoms and their bond breakage. The phase-transition temperature is different for every material as for graphene (4510K), h-BN (3246K), 2H-SiC (4050K), Borophene (2273K), Aluminene (933K), and for 2h-MoS_2 (1460K). The material with greater transition temperature is more stable and can resist the temperature variations up-to that temperature. the energy values again start increasing linearly after phase-transition, depicting their completely molten phase. These energy values continue increasing until next transition.

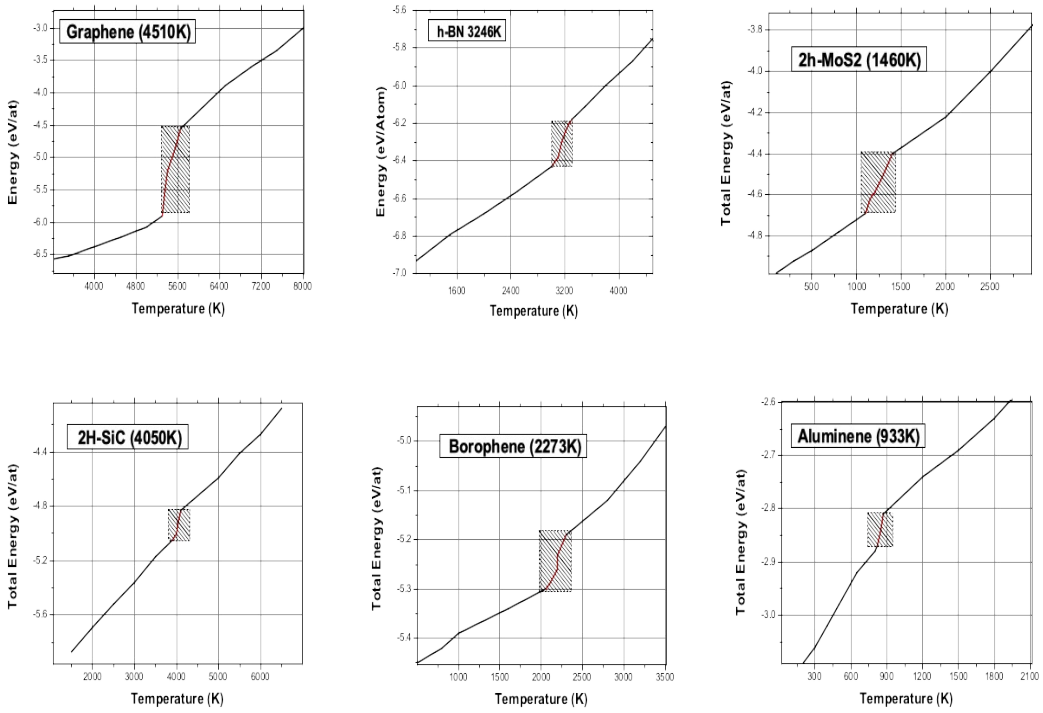

Figure 7: Temperature dependent energy graphs for Germanene, Graphene, h-BN, 2h-MoS_2 2-SiC, Borophene, and Aluminene.

4. Conclusions

A detailed study was carried out to investigate the structural and thermal stability of compound as well as elemental 2D-mono-layered slabs using Molecular-Dynamics simulations. The optimized structural parameters lattice-constants and bond-lengths agreed with literature. The findings of this work are based on determining the thermal stability of the slabs through Radial-Distribution-Function (RDF). Thermal stability was compared by plotting the temperature and energy curves from which, the phase transition temperature and heat capacity were inferred for all slabs including Graphene, 2H-SiC, h-BN, Borophene, Germanene, 2h-MoS_2 and Aluminene. Their phase transition temperatures correspond to 4510 K, 4050 K, 3246 K, 2273 K, 1670 K, 1460 K and 933 K respectively predicting the trend of most to least thermally stable material. The FWHM was calculated which provides the information about thermal broadening of RDF-Peaks of all elemental monolayers.

5. Acknowledgement

The authors extend their sincere appreciation to the Deanship of Scientific Research at King Saud University for funding this work through research group no. RG-1441-384.

References

Ahadi, Z., Shadman Lakmehsari, M., Kumar Singh, S., & Davoodi, J. (2017). Stability and thermal behavior of molybdenum disulfide nanotubes: Nonequilibrium molecular dynamics simulation using REBO potential. *Journal of Applied Physics, 122*(22), 224303.

Aktulga, H. M., Pandit, S. A., van Duin, A. C., & Grama, A. Y. (2012). Reactive molecular dynamics: Numerical methods and algorithmic techniques. *SIAM Journal on Scientific Computing, 34*(1), C1-C23.

Balandin, A. A., Ghosh, S., Bao, W., Calizo, I., Teweldebrhan, D., Miao, F., & Lau, C. N. (2008). Superior thermal conductivity of single-layer graphene. *Nano letters, 8*(3), 902-907.

Balendhran, S., Walia, S., Nili, H., Sriram, S., & Bhaskaran, M. (2015). Elemental analogues of graphene: silicene, germanene, stanene, and phosphorene. *small, 11*(6), 640-652.

Blake, P., Hill, E., Castro Neto, A., Novoselov, K., Jiang, D., Yang, R., . . . Geim, A. (2007). Making graphene visible. *Applied Physics Letters, 91*(6), 063124.

Cahangirov, S., Topsakal, M., Aktürk, E., Şahin, H., & Ciraci, S. (2009). Two-and one-dimensional honeycomb structures of silicon and germanium. *Physical review letters, 102*(23), 236804.

Chen, Y., Xi, J., Dumcenco, D. O., Liu, Z., Suenaga, K., Wang, D., . . . Xie, L. (2013). Tunable band gap photoluminescence from atomically thin transition-metal dichalcogenide alloys. *ACS nano, 7*(5), 4610-4616.

Dávila, M., Xian, L., Cahangirov, S., Rubio, A., & Le Lay, G. (2014). Germanene: a novel two-dimensional germanium allotrope akin to graphene and silicene. *New Journal of Physics, 16*(9), 095002.

Davydov, S. Y. (2010). Elastic properties of graphene: The Keating model. *Physics of the Solid State, 52*(4), 810-812.

Feng, B., Zhang, J., Zhong, Q., Li, W., Li, S., Li, H., . . . Wu, K. (2016). Experimental realization of two-dimensional boron sheets. *Nature chemistry, 8*(6), 563-568.

Frenkel, D., & Smit, B. (2002). Understanding molecular simulation: From algorithms to applications (Vol. 1, pp. 1-638): Elsevier (formerly published by Academic Press).

Ganz, E., Ganz, A. B., Yang, L.-M., & Dornfeld, M. (2017). The initial stages of melting of graphene between 4000 K and 6000 K. *Physical Chemistry Chemical Physics, 19*(5), 3756-3762.

Geim, A. K., & Novoselov, K. S. (2010). The rise of graphene *Nanoscience and technology: a collection of reviews from nature journals* (pp. 11-19): World Scientific.

Giang, N. H., Tran, T. T. H., & Van Hoang, V. (2019). Structural and thermodynamic properties of two-dimensional confined germanene: a molecular dynamics and DFT study. *Materials Research Express, 6*(8), 086411.

Giang, N. H., Van Hoang, V., & Hanh, T. T. T. (2020). Melting of two-dimensional perfect crystalline and polycrystalline germanene. *Physica E: Low-dimensional Systems and Nanostructures, 119*, 114021.

Golberg, D., Bando, Y., Huang, Y., Terao, T., Mitome, M., Tang, C., & Zhi, C. (2010). Boron nitride nanotubes and nanosheets. *ACS nano, 4*(6), 2979-2993.

Hernandez, E., Goze, C., Bernier, P., & Rubio, A. (1998). Elastic properties of C and B x C y N z composite nanotubes. *Physical review letters, 80*(20), 4502.

Hill, E. W., Geim, A. K., Novoselov, K., Schedin, F., & Blake, P. (2006). Graphene spin valve devices. *IEEE transactions on magnetics, 42*(10), 2694-2696.

Huang, Y., Zhuge, F., Hou, J., Lv, L., Luo, P., Zhou, N., . . . Zhai, T. (2018). Van der Waals coupled organic molecules with monolayer MoS2 for fast response photodetectors with gate-tunable responsivity. *ACS nano, 12*(4), 4062-4073.

Kamal, C., Chakrabarti, A., & Ezawa, M. (2015). Aluminene as highly hole−doped graphene. *New Journal of Physics, 17*(8), 083014.

Kou, L., Frauenheim, T., & Chen, C. (2014). Phosphorene as a superior gas sensor: selective adsorption and distinct I–V response. *The journal of physical chemistry letters, 5*(15), 2675-2681.

Kroto, H. (1990). Fullerene cage clusters. The key to the structure of solid carbon. *Journal of the Chemical Society, Faraday Transactions, 86*(13), 2465-2468.

Lebegue, S., & Eriksson, O. (2009). Electronic structure of two-dimensional crystals from ab initio theory. *Physical Review B, 79*(11), 115409.

Lherbier, A., Botello-Méndez, A. R., & Charlier, J.-C. (2016). Electronic and optical properties of pristine and oxidized borophene. *2D Materials, 3*(4), 045006.

Li, W., Yang, Y., Zhang, G., & Zhang, Y.-W. (2015). Ultrafast and directional diffusion of lithium in phosphorene for high-performance lithium-ion battery. *Nano letters, 15*(3), 1691-1697.

Lin, X., Lin, S., Xu, Y., Hakro, A. A., Hasan, T., Zhang, B., . . . Chen, H. (2013). Ab initio study of electronic and optical behavior of two-dimensional silicon carbide. *Journal of Materials Chemistry C, 1*(11), 2131-2135.

Liu, H., Neal, A. T., Zhu, Z., Luo, Z., Xu, X., Tománek, D., & Ye, P. D. (2014). Phosphorene: an unexplored 2D semiconductor with a high hole mobility. *ACS nano, 8*(4), 4033-4041.

Ma, N., Reis, M.S., (2017) Barocaloric effect on graphene. *Sci Rep* **7,** 13257.

Mukhopadhyay, G., & Behera, H. (2013). Emerging Two-dimensional Materials: graphene and its other structural analogues. *arXiv preprint arXiv:1306.0809*.

Neto, A. C., Guinea, F., Peres, N. M., Novoselov, K. S., & Geim, A. K. (2009). The electronic properties of graphene. *Reviews of modern physics, 81*(1), 109.

Ostadhossein, A., Rahnamoun, A., Wang, Y., Zhao, P., Zhang, S., Crespi, V. H., & Van Duin, A. C. (2017). ReaxFF reactive force-field study of molybdenum disulfide (MoS2). *The journal of physical chemistry letters, 8*(3), 631-640.

Pan, L., Liu, H., Wen, Y., Tan, X., Lv, H., Shi, J., & Tang, X. (2011). First-principles study of monolayer and bilayer honeycomb structures of group-IV elements and their binary compounds. *Physics Letters A, 375*(3), 614-619.

Patti, A. (2010). Molecular Modeling of Self-assembling Hybrid Materials (PhD Thesis). *arXiv preprint arXiv:1006.0945*.

Peng, B., Zhang, H., Shao, H., Ning, Z., Xu, Y., Ni, G., . . . Zhu, H. (2017). Stability and strength of atomically thin borophene from first principles calculations. *Materials Research Letters, 5*(6), 399-407.

Ranjan, P., Sahu, T. K., Bhushan, R., Yamijala, S. S., Late, D. J., Kumar, P., & Vinu, A. (2019). Freestanding borophene and its hybrids. *Advanced Materials, 31*(27), 1900353.

Şahin, H., Cahangirov, S., Topsakal, M., Bekaroglu, E., Akturk, E., Senger, R. T., & Ciraci, S. (2009). Monolayer honeycomb structures of group-IV elements and III-V binary compounds: First-principles calculations. *Physical Review B, 80*(15), 155453.

Shi, Z., Zhang, Z., Kutana, A., & Yakobson, B. I. (2015). Predicting two-dimensional silicon carbide monolayers. *ACS nano, 9*(10), 9802-9809.

Sun, X., Dai, J., Guo, Y., Wu, C., Hu, F., Zhao, J., . . . Xie, Y. (2014). Semimetallic molybdenum disulfide ultrathin nanosheets as an efficient electrocatalyst for hydrogen evolution. *Nanoscale, 6*(14), 8359-8367.

Thomas, S., Ajith, K., Chandra, S., & Valsakumar, M. (2015). Temperature dependent structural properties and bending rigidity of pristine and defective hexagonal boron nitride. *Journal of Physics: Condensed Matter, 27*(31), 315302.

Vogt, P., De Padova, P., Quaresima, C., Avila, J., Frantzeskakis, E., Asensio, M. C., . . . Le Lay, G. (2012). Silicene: compelling experimental evidence for graphenelike two-dimensional silicon. *Physical review letters, 108*(15), 155501.

Wallace, P. R. (1947). The band theory of graphite. *Physical review, 71*(9), 622.

Wang, J., Ma, F., Liang, W., & Sun, M. (2017). Electrical properties and applications of graphene, hexagonal boron nitride (h-BN), and graphene/h-BN heterostructures. *Materials Today Physics, 2*, 6-34.

Wang, J., Ma, F., & Sun, M. (2017). Graphene, hexagonal boron nitride, and their heterostructures: properties and applications. *RSC advances, 7*(27), 16801-16822.

Wang, Q., Kalantar-Zadeh, K., & Kis, A. (2012). Coleman. JN & Strano, MS. *Nature Nanotech, 7*, 699-712.

Wypych, F., & Schöllhorn, R. (1992). 1T-MoS 2, a new metallic modification of molybdenum disulfide. *Journal of the Chemical Society, Chemical Communications*(19), 1386-1388.

Yang, G., Li, L., Lee, W. B., & Ng, M. C. (2018). Structure of graphene and its disorders: a review. *Science and Technology of advanced MaTerialS, 19*(1), 613-648.

Yang, X., Ding, Y., & Ni, J. (2008). Ab initio prediction of stable boron sheets and boron nanotubes: structure, stability, and electronic properties. *Physical Review B, 77*(4), 041402.

Yoon, K., Ostadhossein, A., & Van Duin, A. C. (2016). Atomistic-scale simulations of the chemomechanical behavior of graphene under nanoprojectile impact. *Carbon, 99*, 58-64.

Yuan, J., & Liew, K. (2014). Structure stability and high-temperature distortion resistance of trilayer complexes formed from graphenes and boron nitride nanosheets. *Physical Chemistry Chemical Physics, 16*(1), 88-94.

Yuan, J., Yu, N., Xue, K., & Miao, X. (2017). Stability, electronic and thermodynamic properties of aluminene from first-principles calculations. *Applied Surface Science, 409*, 85-90.

Zhang, Z., Yang, Y., Gao, G., & Yakobson, B. I. (2015). Two−dimensional boron monolayers mediated by metal substrates. *Angewandte Chemie, 127*(44), 13214-13218.

Zhi, C., Bando, Y., Tang, C., Kuwahara, H., & Golberg, D. (2009). Large−scale fabrication of boron nitride nanosheets and their utilization in polymeric composites with improved thermal and mechanical properties. *Advanced Materials, 21*(28), 2889-2893.

Figure 1: The optimized structure of buckled germanene viewed along (a) z-axis, (b) y-axis and (c) x-axis. The calculated values of bond length and buckling width are shown.

Figure 2: The optimized structures of Aluminene, 2h-MoS2, Borophene, Graphene, h-BN, and 2D-SiC viewed along x-axis

Figure 3: RDF-peaks of mono-layered compound materials as a function of interatomic distance between atoms of (a,b,c) 2D-SiC at temperature ranges from 100 to 4500 K (d,e,f) h-BN at temperature ranges from 100 to 3000 K (g,h,i) 2h-MoS_2 at temperature ranges from 300 to 3000 K

Figure 4: RDF- peaks of Germanene as a function of inter-atomic distance (r) at x-axis and probability G(r) at y-axis

Figure 5: RDF-peaks of mono-layered elemental materials as a function of interatomic-distance of (a) Graphene at temperature ranges from 100 to 6000 K (b) Borophene at temperature ranges from 100 to 3000 K and (c) Aluminene at temperature ranges from 100 to 1000 K

Figure 6: Temperature dependent energy values and their corresponding graph for Germanene.

Figure 7: Temperature dependent energy graphs for Germanene, Graphene, h-BN, 2h-MoS_2 2-SiC, Borophene, and Aluminene.